https://doi.org/10.5194/essd-2024-618
Preprint. Discussion started: 21 January 2025
© Author(s) 2025. CC BY 4.0 License.

Open Access Earth System Science Data Discussions

Mapping global distributions, environmental controls, and uncertainties of apparent top- and subsoil organic carbon turnover times

Lei Zhang[1,2], Lin Yang[1], Thomas W. Crowther[3], Constantin M. Zohner[3], Sebastian Doetterl[4], Gerard B.M. Heuvelink[5,6], Alexandre M.J.-C. Wadoux[7], A-Xing Zhu[8], Yue Pu[1], Feixue Shen[1], Haozhi Ma[9], Yibiao Zou[3], Chenghu Zhou[1,10]

[1] School of Geography and Ocean Science, Nanjing University, Nanjing, China
[2] Climate and Ecosystem Science Division, Lawrence Berkeley National Laboratory, Berkeley, CA, USA
[3] Institute of Integrative Biology, ETH Zurich (Swiss Federal Institute of Technology), Zurich, Switzerland
[4] Soil Resources Group, Department of Environmental Systems Science, ETH, Zurich, Switzerland
[5] Soil Geography and Landscape Group, Wageningen University, Wageningen, The Netherlands
[6] ISRIC – World Soil Information, Wageningen, The Netherlands
[7] LISAH, Univ Montpellier, AgroParisTech, INRAE, IRD, L'Institut Agro, Montpellier, France
[8] Department of Geography, University of Wisconsin-Madison, Madison, WI, USA
[9] Swiss Federal Institute for Forest, Snow and Landscape Research WSL, Birmensdorf, Switzerland
[10] State Key Laboratory of Resources and Environmental Information System, Institute of Geographical Sciences and Natural Resources Research, Chinese Academy of Sciences, Beijing, China

Correspondence to: Lin Yang (yanglin@nju.edu.cn) and Chenghu Zhou (zhouch@lreis.ac.cn)

Abstract. The turnover time (τ) of global soil organic carbon is central to the functioning of terrestrial ecosystems. Yet our spatially-explicit understanding of depth-dependent variations and environmental controls of τ at a global scale remain incomplete. In this study, we combine multiple state-of-the-art observation-based datasets, including over ninety thousand geo-referenced soil profiles, the latest root observations distributed globally, and large amounts of satellite-derived environmental variables, to generate global maps of apparent τ in topsoil (0–0.3 m) and subsoil (0.3–1 m) layers with a spatial resolution of 30 arcsec (~1 km at the Equator). We show that subsoil τ (385^{3485}_{20} years [mean with a variation range from 2.5th to 97.5th percentile]) is over eight times longer than topsoil τ (15^{137}_{11} years). The cross-validation shows that the fitted machine learning models effectively captured the variabilities in τ, with R^2 values of 0.87 and 0.70 for topsoil and subsoil τ mapping, respectively. The prediction uncertainties of the τ maps were quantified for better user applications. The environmental controls on top- and subsoil τ were investigated at global, biome, and local scales. Our analyses illustrate that how temperature, water availability, physio-chemical properties and depth exert jointly impacts on τ. The data-driven approaches allow us to identify their interactions, thereby enriching our comprehension of mechanisms driving nonlinear τ–environment relationships from global to local scales. The distributions of dominating factors of τ at local scales were mapped for identifying context-dependent controls on τ across different regions. We further reveal that the current Earth system models may underestimate τ by comparing model-derived maps with our observation-derived τ maps. The resulting maps with new insights demonstrated in this study facilitate the future modelling efforts of carbon cycle–climate feedbacks and supporting effective carbon management. The dataset is archived and freely available at https://doi.org/10.5281/zenodo.14560239 (Zhang, 2025).

https://doi.org/10.5194/essd-2024-618
Preprint. Discussion started: 21 January 2025
© Author(s) 2025. CC BY 4.0 License.

Open Access Earth System Science Data Discussions

1 Introduction

As the largest active reservoir of organic carbon in terrestrial ecosystems, soils are integral to the global carbon cycle (Schimel, 1995; Batjes, 1996; Smith et al., 2024). Plants capture CO_2 from the atmosphere through photosynthesis and transfer carbon into soils through litter fall and root exudates. This carbon is then cycled back to the atmosphere through heterotrophic respiration by organic-matter decomposers, a process governed by decomposition rates (Balesdent et al., 2018). The turnover time of soil organic carbon (SOC), denoted as τ (in years), is the average time that organic carbon molecules remain in the soil (Six and Jastrow, 2002; Sierra et al., 2017). This turnover time is a critical factor in determining the size of soil carbon pools (Sierra et al., 2017; Crowther et al., 2019b). Understanding the spatial variation in τ and the underlying environmental drivers is therefore crucial for comprehending the scale and dynamics of terrestrial carbon storage under current and future climate change scenarios (Torn et al., 2009; Field et al., 2014).

Several studies have estimated the global apparent carbon turnover times in whole terrestrial ecosystems (Carvalhais et al., 2014; Fan et al., 2020). Nevertheless, the detailed patterns of τ in soil systems at the global scale remain to be elucidated. Much work has focused on shallow soil horizons as the higher carbon content and the greater availability of data in topsoils (e.g., Crowther et al., 2016; Luo et al., 2017; Viscarra Rossel et al., 2019; Wu et al., 2021). However, capturing the biogeographic variability of carbon dynamics in deeper soil layers is emerging as a critical area of research (Hicks Pries et al., 2023), as the environmental sensitivities of SOC there can substantially differ from surface layers (Rumpel and Kögel-Knabner, 2011; Hicks Pries et al., 2017; Luo et al., 2019; Soong et al., 2021; Zosso et al., 2023). To enhance our understanding of soil carbon turnover and address these issues, there is a clear need for a global analysis of τ that considers both top- and subsoil layers, and providing spatially-explicit τ maps. Such an analysis should leverage the latest and most comprehensive global soil profile datasets available, enabling more reliable assessments and insights into terrestrial carbon sink potential.

The ensemble of latest datasets also supports a more nuanced understanding of the environmental controls on τ, particularly for their potentially non-linear or distinct effects across different spatial scales and soil depths. Previous studies showed evidence that the turnover time of SOC is negatively correlated with temperature and precipitation (Davidson and Janssens, 2006; Chen et al., 2013; Wang et al., 2018), and that subsoil carbon may be particularly sensitive to temperature fluctuations (Jia et al., 2019; Soong et al., 2021; Chen et al., 2023). Yet, other studies could not confirm this strong climatic dependency (Giardina and Ryan, 2000; Doetterl et al., 2015), suggesting a predominant influence of soil properties on subsoil carbon turnover times in certain regions or over decadal timescales (Luo et al., 2019). This inconsistency underscores the need for a multifaceted approach to quantify the effects of multiple factors on τ, particularly the interactions between climate and edaphic factors, across different spatial scales and soil depths (Schmidt et al., 2011). Comprehensive assessments at the global, biome, and local levels will be crucial to identify the primary controls of τ for both topsoil and subsoil layers. Moreover, observation-based global estimates of τ are essential for simulating the global carbon cycle (Todd-Brown et al., 2013; Friend et al., 2014; Varney et al., 2022). An accurate representation and deeper understanding of the

https://doi.org/10.5194/essd-2024-618
Preprint. Discussion started: 21 January 2025
© Author(s) 2025. CC BY 4.0 License.

environmental controls of τ – spanning diverse spatial scales and soil depths – will be integral to benchmarking current Earth system models (ESMs) and reducing bias in future carbon cycle projections.

This study aims to develop a global estimation of τ by integrating the state-of-the-art soil and root profile databases with satellite-derived environmental observations. The collected datasets allow us to firstly estimate τ at over ninety thousand global sampling sites, and then we used machine learning methods to generate a spatially-explicit understanding of global SOC turnover times in the top- (0–0.3 m) and subsoil (0.3–1 m). To comprehend the interactive mechanisms among multiple environmental drivers that have shaped variations in top- and subsoil τ at the global, biome-level and local scales, we used data-driven approaches to characterized the directional contributions of climate, topography, physical and chemical properties of soil to explain τ patterns. We further quantified the uncertainty maps for better user applications, and compared our observation-derived τ with ESM-derived τ in both spatial variabilities and climatic dependencies.

2 Materials and methods

2.1 Estimation of τ in top- and subsoil layers

The SOC turnover time (τ) we estimated in this study is the mean transit time that the newly entered carbon spends in soils until it leaves (Six and Jastrow, 2002; Sierra et al., 2017). When assuming a steady state and homogeneity of the system in which all particles have the same probability of leaving at any time, τ can be defined as the ratio between SOC stock (SOCS) to input or output flux of carbon ($\tau = SOCS/flux$), which can be called the apparent turnover time (Carvalhais et al., 2014; Fan et al., 2020). We estimated SOC stock (see Section 2.1.1) and vertical allocation of carbon input in two soil layers (see Section 2.1.2), and then combined them to calculate top- and subsoil τ at all soil profile locations. We then adopted the point-level estimates to map τ variation across the globe.

2.1.1 Estimation of SOC stocks based on soil sample databases

Soil sample data were mainly collected form the standardized soil profile database provided by World Soil Information Service (WoSIS) (Batjes et al., 2020). The Northern Circumpolar Soil Carbon Database (NCSCD) (Hugelius et al., 2013) was incorporated to supplement samples across the high latitudes of the Northern Hemisphere. In addition, the soil sample data from the project of National Soil Survey of China was incorporated (Zhang et al., 2013; Liu et al., 2022). To minimize bias due to erroneous and/or uncertain measurements, we removed samples i) with low accuracy of the geographical coordinates (i.e., the information of degree, minute and second is not fully provided in the source), ii) located in areas with exceptionally low NPP (below 10 gC m^{-2} yr^{-1}), iii) with low quality of NPP estimates (if the quality control value is larger than 50%), and iv) layer observations flagged as surficial litter. Finally, a total number of 95,200 and 66,807 geo-referenced sampling locations providing topsoil and subsoil information were collected for this study (Fig. 1). The estimation of SOC

https://doi.org/10.5194/essd-2024-618
Preprint. Discussion started: 21 January 2025
© Author(s) 2025. CC BY 4.0 License.

stock (SOCS, kgC m^{-2}) for each soil sample site at a certain depth interval between the upper depth (D_u, m) and lower depth (D_l, m) can be computed as follows:

$$\mathrm{SOCS}_{D_u-D_l} = \mathrm{SOC}_{D_u-D_l} \cdot \mathrm{BD} \cdot \left(1 - \frac{\mathrm{CF}}{100}\right) \cdot (D_u - D_l) \quad (1)$$

Were the BD is the soil bulk density (g cm^{-3}), and CF is the percentage of coarse fragments in the whole soil (%). We adopted an approach described in Text S1 to fill the missing values by using a specific pedotransfer function depending on the SOC content and the considered layer. When CF was missing, we extracted the corresponding data at their locations from the latest version of SoilGrids maps (Poggio et al., 2021). The equal-area spline algorithm was employed to fit layers observations at different depth intervals (Bishop et al., 1999; Malone et al., 2009). The average of fitted values were adopted to estimate the SOCS at two layers for each profile (Figs. S1). The probability distributions of SOCS, BD, and CF in different biomes are shown in Figs. S2-S4.

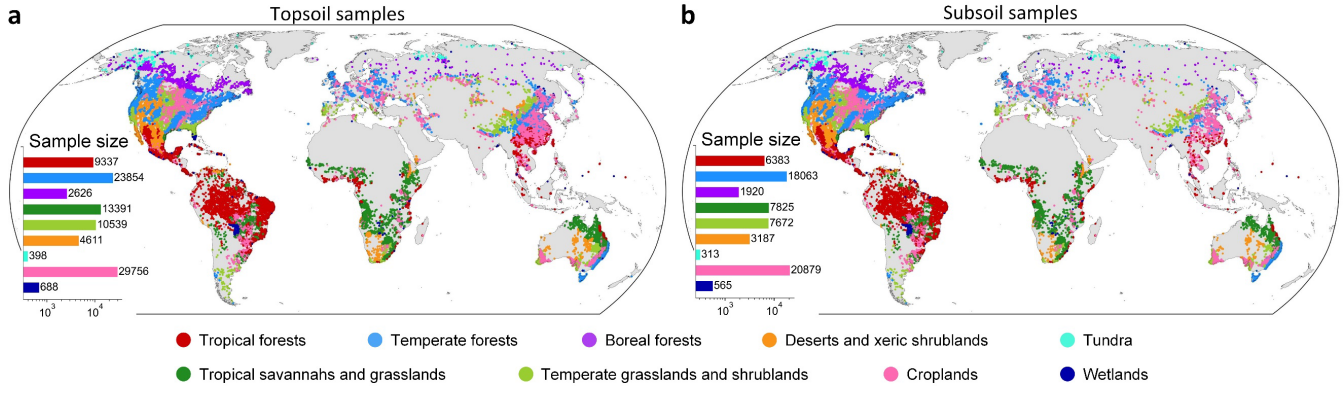

Figure 1: Spatial distributions of geo-referenced soil samples used in the study across global biomes. A total of 95,200 (**a**, for topsoil) and 66,807 (**b**, for subsoil) sampling sites were collected from multiple soil profile databases. The bar plots show the sample size within each biome.

2.1.2 Estimation of carbon allocation belowground

The flux of carbon at a certain soil layer needs to be obtained through vertical allocation of the amount of net primary productivity (NPP). This involves the estimations of above- and belowground NPP and NPP allocation into different soil layers. The annual NPP (kgC m^{-2} yr^{-1}) produced by the moderate-resolution imaging spectroradiometer (MODIS) was collected at each sample location (Running and Zhao, 2019). The mean of annual NPP from 2001 to 2019 was computed for representing the general status of each sample location. Then, we used the biomass ratio between roots and shoots (root-to-shoot ratio, RSR) as a proxy to estimate the amount of NPP allocated to soils, as it is generally a realistic estimation for the mean long-term NPP partitioning (Gower et al., 1999). The fraction of belowground NPP can be estimated as the root-mass fraction (RMF):

https://doi.org/10.5194/essd-2024-618
Preprint. Discussion started: 21 January 2025
© Author(s) 2025. CC BY 4.0 License.

$$\mathrm{RMF} = \frac{\mathrm{RSR}}{\mathrm{RSR} + 1} \tag{2}$$

The RSR value at each sample location was collected from the harmonized global maps of above and belowground biomass carbon density (Spawn et al., 2020). The biome-specific variabilities of RMF are shown in Fig. S5.

We used the vertical root biomass distribution to represent the belowground NPP partitioned into different soil depths (Luo et al., 2019; Xiao et al., 2022, 2023). The root distribution information was obtained from the global 564 root profiles complied by Schenk and Jackson (Schenk and Jackson, 2002). The logistic dose–response curve function was used to estimate the cumulative amount of root mass $r(D)$ above a certain soil depth D (m):

$$r(D) = \frac{R_{max}}{1 + \left(\frac{D}{D_{50}}\right)^{c}} \tag{3}$$

where R_{max} represents the total amount of roots, D_{50} is the depth at which $r(D)$ equals to the half of R_{max}, and c is a dimensionless shape-parameter which can refer to Schenk and Jackson (2002) for details. The fraction of roots in a certain soil layer between D_u and D_l ($fr_{D_u-D_l}$) can be estimated as follows:

$$fr_{D_u-D_l} = \frac{r_{D_l}}{R_{max}} - \frac{r_{D_u}}{R_{max}} = \frac{1}{1 + \left(\frac{D_l}{D_{50}}\right)^{c}} - \frac{1}{1 + \left(\frac{D_u}{D_{50}}\right)^{c}} \tag{4}$$

This root profile dataset has been used to analyze the belowground NPP allocation in several previous studies (Luo et al., 2019; Shi et al., 2021). In our study, we extended this data by collecting the latest Root Systems of Individual Plants (RSIP) database and the global root traits (GRooT) database that includes the information of the maximum belowground extents of terrestrial plants (Guerrero-Ramírez et al., 2021; Tumber-Dávila et al., 2022). By assuming that the root distribution is proportional to its morphological distribution (Bardgett et al., 2014; Tumber-Dávila et al., 2022), we used the form trait of root, the maximum rooting depth (D_{max}), to generate an alternative representation of the root distribution. A total of 1,732 geo-referenced measurements were collected with description of rooting depth from those two databases. The vertical root distribution can be estimated according to a commonly used asymptotic equation (Gale and Grigal, 1987; Jackson et al., 1996; Zeng, 2001):

$$CRF(D) = 1 - \beta^{D} \tag{5}$$

where CRF is the cumulative root fraction from the surface to soil depth D in centimeters, β is the estimated parameter which controls the decreasing rate of root mass with increasing soil depth (Gale and Grigal, 1987; Zeng, 2001). Finally, the fraction of roots in a certain soil layer between upper and lower depth ($fr_{D_u-D_l}$) can be quantified as: $CRF(D_l) - CRF(D_u)$. An illustration of the root distribution estimation through the above approach is shown in Fig. S6.

https://doi.org/10.5194/essd-2024-618
Preprint. Discussion started: 21 January 2025
© Author(s) 2025. CC BY 4.0 License.

Open Access Earth System Science Data Discussions

Hence, the global distributions of all root profiles that characterize the fraction of root in two layers were calculated and are shown in Fig. S7. Given that root distribution is generally related with the biome, vegetation type and soil conditions (Jackson et al., 1996; Schenk and Jackson, 2005), for each soil sample site, root profile observations within the same terrestrial ecoregions (Dinerstein et al., 2017) and the same soil type (FAO–Unesco, 1990) as that of the soil sample were selected. The corresponding mean fr of those selected root observations for each soil sample locations were finally collected (Figs. S8 and S9).

The vertically physical transportation of organic carbon, such as leaching and/or bioturbation, is also necessary to be considered. We followed the function designed in previous model that includes vertical transport of SOC (Braakhekke et al., 2011; Koven et al., 2013; Sierra et al., 2024):

$$V(D) = Diff\frac{\partial^2 C}{\partial D^2} \tag{6}$$

where V is the transported SOC stock (V) in a certain layer; C is the organic carbon content, which is defined volumetrically (kg m^{-3}), at the depth D; $Diff$ is the diffusivity which is constant and set to be 1×10^{-4} m^2 $year^{-1}$ according previous studies (Koven et al., 2013; Sierra et al., 2024). Thus, the belowground NPP (BNPP) in a certain soil layer can be estimated as follows:

$$\mathrm{BNPP}_{D_u-D_l} = \mathrm{NPP}\cdot\mathrm{RMF}\cdot fr_{D_u-D_l} + V_{D_u-D_l} \tag{7}$$

For topsoil, carbon inputs also contain a portion of carbon from surface litterfall, which should be additionally considered. First, the RSR dataset was adopted to support us to obtain the aboveground NPP (ANPP). As a decent fraction of NPP was removed as the harvest products in croplands, we performed a specific calculation procedure to estimate the aboveground carbon input in this region as described in Text S2. Second, we used two databases including measurements of aboveground litterfall across the globe (Holland et al., 2015; Jia et al., 2016), to estimate the fraction of aboveground NPP (ANPP) converted into litterfall. Then, we determined the fraction of litterfall allocated as the carbon input to topsoil according to the decomposition processes described in Community Land Model (Oleson et al., 2013). The details of calculations related with the fraction of ANPP that transferred as carbon input into the topsoil (denoted as fr_a) are described in Text S3.

Therefore, the carbon input flux between upper (D_u) and lower depth (D_l) can be estimated as follows (the biome-specific variabilities of this variable are shown in Fig. S10):

$$\mathrm{flux}_{D_u-D_l} = \mathrm{BNPP}_{D_u-D_l} + fr_a\cdot\mathrm{ANPP} \tag{8}$$

Combining the estimated SOC stock (Eq. 1) and carbon allocation belowground (Eq. 8) with the equation of apparent τ, the values of τ in top- and subsoil layers were calculated at all sample locations across the globe are shown in Fig. S11. Table S1 shows the details of datasets used to calculate τ for all samples.

https://doi.org/10.5194/essd-2024-618
Preprint. Discussion started: 21 January 2025
© Author(s) 2025. CC BY 4.0 License.


2.2 Geospatial mapping of τ

The machine learning-based method was adopted to generate the spatially explicit maps of τ at the two soil layers. As the procedure of geospatial predictive mapping illustrated in Fig. S12, we used the random forest (RF) model to establish the relationship between τ and it potentially related geographical variables (i.e., environmental covariates), for mapping the global distribution of τ with quantification of uncertainty. The advantage of RF is the incorporation of randomized feature selection and training sample selection (Breiman, 2001), so that it can reduce the overfitting risk and lead to a good ability for generalization. This model has been effectively applied on large datasets for geospatial mapping tasks at the global scale (van den Hoogen et al., 2019; Ma et al., 2021; Poggio et al., 2021). The covariates including climate, soil physical, soil chemical properties and topography were collected (Table S2 and Figs. S13-S18). These covariate maps were overlaid and thus allowed us to predict τ at the global scale with a spatial resolution of 30 arc-seconds (~1 km^2 at the Equator). Considering some regions covered by organic soils, such as peatlands, cannot be well represented when using our method to generate estimations, therefore, we masked these regions according to the definition of organic soil in Brady & Weil (1999).

2.3. Analysis of environmental controls

To investigate the environmental controls of the spatial distribution of τ at two layers, the RF model was adopted based on all soil sample data to quantify the relative importance (*RI*) of each covariate at the global scale. We used permutation-based feature importance as the metric to assess *RI* (Altmann et al., 2010) (see Text S4).

The directional effects of important environmental factors on τ was investigated by using the partial regression model to calculate the partial correlations of top- and subsoil τ with the six top ranked environmental variables from RF modelling mentioned above. The analyzed variables are mean annual temperature (MAT) and precipitation (MAP), the fine particle-size fraction (CLAY+SILT), organic carbon to total nitrogen ratio (C:N), cation exchange capacity of the soil (CEC), and soil pH. The partial correlation of each influencing factor was calculated while controlling other factors.

Given the potentially non-significant effects of a variable (e.g. the global impact of precipitation) on τ in a global-level linear model, it does not necessarily imply that the respective variable has no influence on τ. Instead, this lack of significance may arise from its divergent effects when interacting with other factors. This led to an interest in exploring the reasons behind such nonlinear and uncoherent driving mechanisms. Considering the extrinsic climate effects on soil carbon turnover can be interacted by regionally intrinsic soil characteristics (Doetterl et al., 2015), we used an approach (see Text S5) to exemplify the interactive effects of MAT and MAP on top- and subsoil τ in response to the changes of other factors (namely interactive factors). In addition to the overall importance of covariates analyzed at the large scale, the local-level importance for four categories of variables was also assessed (see Text S6).

https://doi.org/10.5194/essd-2024-618
Preprint. Discussion started: 21 January 2025
© Author(s) 2025. CC BY 4.0 License.

2.4 Evaluation of mapping results

2.4.1 Assessment of accuracy by cross-validation

The mapping accuracy was assessed by using a 10-fold cross validation. The total sample data were divided into ten equally sized subsets, and this division was performed on each biome data to ensure that the ten split sets can keep a balance among biomes. Nine folds were used as the training data to fit the model, and the prediction was validated on the one remaining fold. This procedure was carried out ten times, and each time using a different fold for validation. The mean value of coefficient-of-determination (R^2) and root mean squared error (RMSE) for all folds were computed as the final accuracy metrics for the assessment of mapping results.

2.4.2 Quantification of uncertainty

To evaluate the uncertainty of predictive maps of τ, we adopted quantile regression forests (QRF) (Meinshausen, 2006) to derive prediction intervals. QRF first fits a random forest model in the usual way. Next it computes quantiles of the conditional distribution of τ at each prediction location by replacing observations by indicator transforms. We used the R package ranger (Wright and Ziegler, 2017) with the function *quantreg* to build QRF models. Using this function, not only the prediction values at each location can be obtained, but also the 0.05 quantile ($q_{0.05}$), 0.50 quantile ($q_{0.50}$) and 0.95 quantile ($q_{0.95}$) can be computed to derive the lower limit, median and upper limit of a symmetric 90% prediction interval. This interval has been also adopted for uncertainty assessment in GlobalSoilMap specifications (Arrouays et al., 2014) and SoilGrids product (Poggio et al., 2021).

The uncertainty from the input data in calculation of τ was also considered. When calculating τ for each sample, four input variables (SOCS, NPP, RMF and $fr_{D_u-D_l}$) introduced uncertainty due to errors in soil measurements and estimation of carbon allocation belowground. Errors in these input variables will propagate to the output of τ estimation. To incorporate the error propagation from these inputs to the uncertainty evaluation, the standard deviation (SD) of each input at each sample location needs to be quantified. Here, as the calculation of τ is a simple arithmetic function, the SD of the estimated τ for each sample can be calculated as follows, when ignoring the cross-correlation among those inputs (Heuvelink, 1998):

$$SD_f = \sqrt{\left(\frac{\partial f}{\partial I_1}\right)^2 {SD_{I_1}}^2 + \left(\frac{\partial f}{\partial I_2}\right)^2 {SD_{I_2}}^2 + \cdots + \left(\frac{\partial f}{\partial I_m}\right)^2 {SD_{I_m}}^2} \quad (9)$$

where SD_f represents the SD of the output value calculated by the function f; I_1, I_2 and I_m represent the first, second, and m-th input variables, respectively. For RMF, we directly used the uncertainty maps provided by ref. (Spawn et al., 2020). The SD of SOCS was obtained from Poggio et al. when SOCS was supplemented by extracting values from SoilGrids maps. For quantifying the SD of $fr_{D_u-D_l}$, the SD of all selected root profile observation values for each soil sample site was adopted to represent its uncertainty. For NPP, considering that most MODIS NPP values are within mean ±1SD of the

https://doi.org/10.5194/essd-2024-618
Preprint. Discussion started: 21 January 2025
© Author(s) 2025. CC BY 4.0 License.

respective values observed from the flux-tower (Reichstein et al., 2002), from which we define the uncertainty of NPP values. The relationships between the estimated values of τ and their corresponding SD for all samples are shown in Fig. S19. After quantifying the SD of the estimated τ at each sample location, a Monte Carlo approach was adopted to incorporate the SD in the estimated τ at each sample. That is, the value of τ at each sample location was randomly drawn 100 times from a normal distribution given the known mean and SD. Then, all generated samples were used to fit a QRF model and produce the uncertainty maps.

To visualize the spatial distribution of the prediction uncertainty, we calculated the prediction interval ratio (PIR) defined as the ratio of the range between lower and upper limits over the median:

$$\mathrm{PIR} = \frac{q_{0.95} - q_{0.05}}{q_{0.50}} \tag{10}$$

We also assessed the quality of the estimated prediction uncertainty through an accuracy plot approach by calculating the prediction interval coverage probability (PICP) (Goovaerts, 2001).

3 Results and discussion

3.1 Accuracy assessment

The cross-validation demonstrated that the machine learning models can effectively capture a substantial proportion of τ variations, achieving R^2 values of 0.87 and 0.70, and RMSE values of 14.60 yr and 175.05 yr for the top- and subsoil τ predictions, respectively (Fig. 2). The relatively higher model performance was found in boreal and tundra areas for topsoil and in grasslands and shrublands in warm regions for subsoil, while low model performance was found in temperate forests and subsoil layer in cropland and wetland areas (Figs. S20 and S21). This is probably because soils in those regions are among the most diverse soil landscapes, compared to pedogenetically similar and more climate driven soils in high latitude regions, and more weathered homogenous soils dominating many tropical lowland areas.

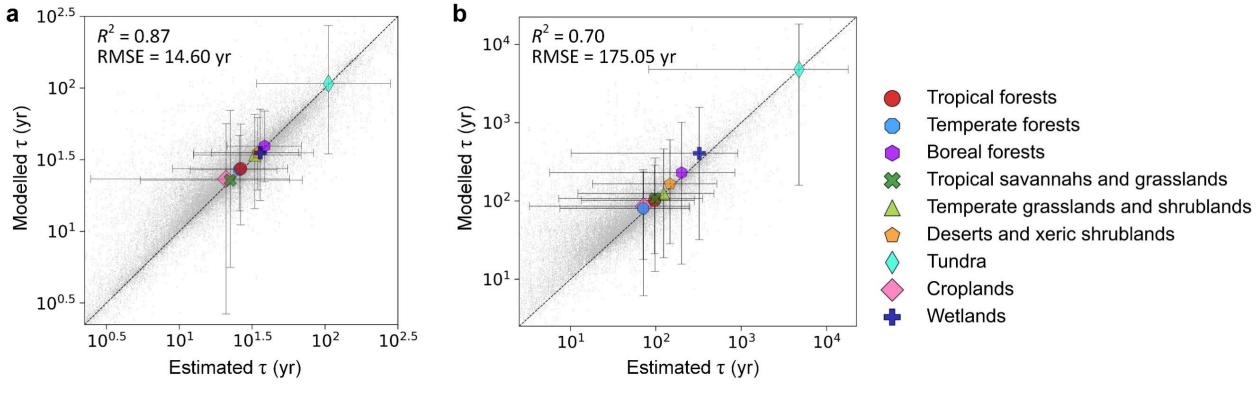

https://doi.org/10.5194/essd-2024-618
Preprint. Discussion started: 21 January 2025
© Author(s) 2025. CC BY 4.0 License.

Figure 2: Validation plots for predictions of soil organic carbon turnover time (τ, yr) at top- (a) and subsoil (b) layer. Predictions were generated using random forest regression models. Grey dots are the estimated τ values based on observations at soil profiles and the predicted values for all validation samples using 10-fold cross-validation. Colored points represent biome-level validation plot. Error bars show 95% percentile intervals of τ in each biome. Black lines indicate the regression lines between predicted and measured values. The shaded grey area represents the. Axes are log10-transformed to account for high skewness of τ.

3.2 Global distributions of τ in top- and subsoil

The spatial-continuous maps of global top- and subsoil τ are shown in Fig. 3. On average, the global τ in the topsoil was 45 yr, ranging from 11 yr (2.5th percentiles) to 137 yr (97.5th percentile). The average subsoil τ was 385 yr, ranging from 20 yr to 3485 yr (Table 1). On a global scale, subsoil SOC turnover time was over eight times longer than that in topsoil. The values of τ generally increased from low to high latitudes, and this latitudinal pattern was more pronounced in the Northern than in the Southern Hemisphere, and it is more evident in the subsoil than in the topsoil layer (Fig. 3b,d). In tropical forests, the average turnover times were shortest, with approximately 25 yr and 74 yr in the top- and subsoil, respectively. The turnover times in temperate, desert and cropland areas for top- and subsoil layers were around 29–43 yr and 78–170 yr, respectively. The longest turnover times were found for tundra regions, with an average longer than 90 yr and 1900 yr for the top- and subsoil layers, respectively. Boreal forests and wetlands also show long carbon turnover times, with an average value of over 50 yr and 500 yr, respectively. As such, the differences in average turnover times between the warmest and coldest biomes were more than 60 years and 1800 years for top- and subsoil layers, respectively.

Table 1. Global- and biome-level statistics of the soil organic carbon turnover time (τ, yr) in top- (0–0.3 m) and subsoil (0.3–1 m) layers.

Global/Biome type	Topsoil τ			Subsoil τ		
	P 2.5	Mean	P 97.5	P 2.5	Mean	P 97.5
Global	11	45	137	20	385	3485
Tropical forests	12	25	46	27	74	155
Temperate forests	15	36	69	17	95	322
Boreal forests	27	58	123	47	530	2569
Tropical savannahs and grasslands	8	31	116	14	101	628
Temperate grasslands and shrublands	10	43	130	18	120	403
Deserts and xeric shrublands	16	43	100	30	170	1250
Tundra	44	91	220	117	1920	7505
Croplands	4	29	64	8	78	204
Wetlands	12	50	187	22	510	5304
Non-permafrost	9	33	82	17	98	377
Permafrost	33	75	188	63	1111	5836

Note: P 2.5 and P 97.5 represent the range of τ in each biome between the 2.5th and 97.5th percentiles from the aggregation of all estimated τ at pixel-level.

https://doi.org/10.5194/essd-2024-618
Preprint. Discussion started: 21 January 2025
© Author(s) 2025. CC BY 4.0 License.

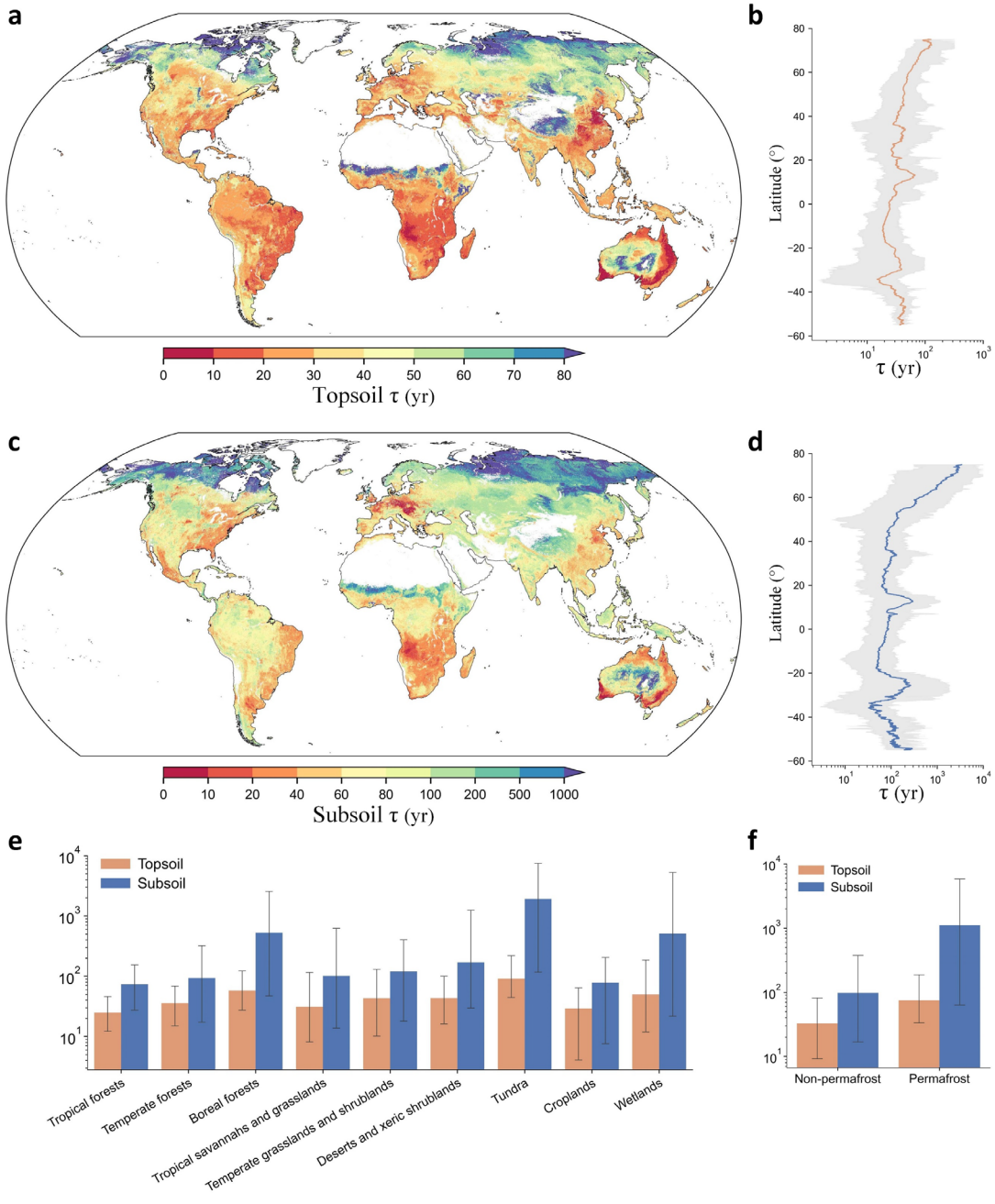

Figure 3: Global patterns of top- and subsoil organic carbon turnover times (τ, yr). Global distributions of τ at top- (0–0.3 m) (**a**) and subsoil (0.3–1 m) (**c**) layers. The predicted maps with a spatial resolution of 30 arcsec (~1 km at the Equator) were generated τ-environment relationships using a machine learning model trained from global soil profile observations and their environmental covariates. **b**, **d**, Latitudinal patterns of top- and subsoil τ. Orange and blue lines represent the average τ at top- and subsoil over latitudes, respectively. The shaded grey areas represent the variations of τ between 2.5th and 97.5th percentiles along latitudes. **e**, **f**, Average τ at two layers in different main biomes. Error bars show the 95% percentile intervals of the spatial predictions within each biome.

https://doi.org/10.5194/essd-2024-618
Preprint. Discussion started: 21 January 2025
© Author(s) 2025. CC BY 4.0 License.

The uncertainty maps quantified for the top- and subsoil are shown in Fig. 4. Uncertainties of subsoil τ predictions were generally higher than that of topsoil τ, likely due to the fewer horizontal observations in the deep layers. Wide prediction intervals were mostly found in areas with low sampling density, such as deserts and permafrost regions. According to the PICP calculation results, the accuracy plots (Fig. S22) show that the proportion of observed τ values in validation set covered in a certain prediction interval approximately equals the size of that probability interval, which validates the unbiased quantification of uncertainty.

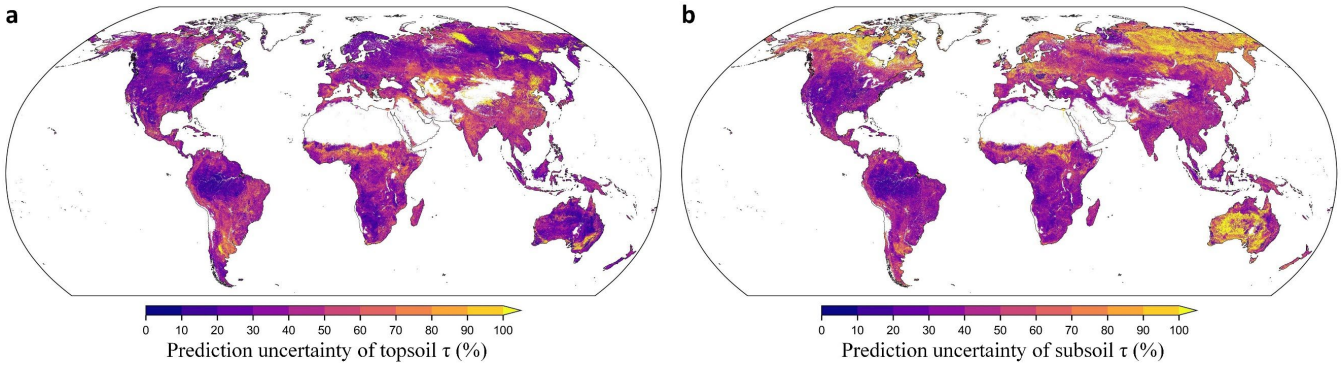

Figure 4: Uncertainty maps of predicted soil organic carbon turnover time (τ) at top- (a) and subsoil (b) layer. The uncertainty was quantified by using quantile regression forests. The values shown in the maps represent the prediction interval ratio (PIR), which is the ratio of the range between lower and upper limit (90% prediction interval bounded by the lower [0.05 quantile] and upper [0.95 quantile] limits) over the median (0.50 quantile) of the predictions.

3.3 Environmental controls of top- and subsoil τ

3.3.1 Global- and biome-level analyses

The relative importance and directional effects of climate, soil (divided into physical and chemical properties) and topographic factors on τ variation at global and biome scales were analyzed (Fig. 5 and Figs. S23, S24). The results suggest scale- and depth-dependency in the drivers of soil turnover times. While climate was found to be the primary driver (explaining nearly half of the total explained variation) of topsoil τ at the global scale, the intrinsic soil characteristics (61%) were more important than climate (32%) for the subsoil τ (Figs. S23a and S24a). This supports recent studies suggesting that soil turnover in deeper layers is less controlled by climatic factors (Luo et al., 2019; Chen et al., 2021; Han et al., 2022) and more by soil properties (Mathieu et al., 2015; Luo et al., 2019). Importantly, by separating soil factors into soil physical (represented by the fine particle-size fraction [CLAY+SILT]) and chemical categories (including C:N, CEC, and soil pH), our study revealed that the topsoil τ is more influenced by soil physical properties than chemical properties (33% *versus* 15%). However, for subsoil τ, soil physical properties are less important than soil chemical properties (27% *versus* 39%). These results support that, in addition to the direct control of climate, pedologic traits and geochemistry of soils exert equivalent or even stronger control on τ at the global scale (Davidson and Janssens, 2006; Doetterl et al., 2015, 2016).

https://doi.org/10.5194/essd-2024-618
Preprint. Discussion started: 21 January 2025
© Author(s) 2025. CC BY 4.0 License.

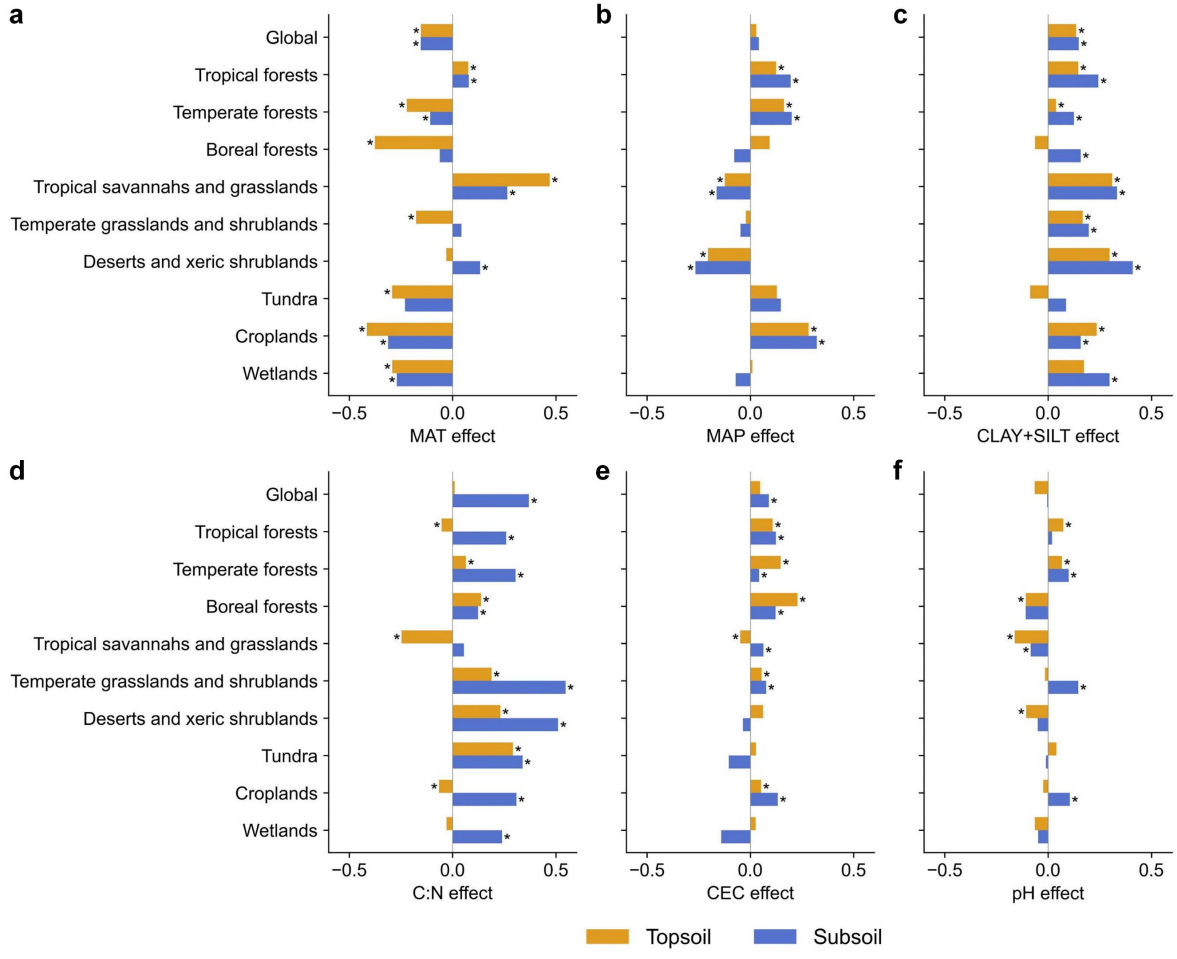

Figure 5: Relationships between environmental variables and soil organic carbon turnover time (τ) in top- and subsoil layers. Effects of six important variables on τ are shown at global and biome levels. Values on bar plots represent coefficients between τ and each variable from partial-regression model, where positive or negative values indicate a positive or negative effect on τ, respectively. MAT: mean annual temperature; MAP: mean annual precipitation; CLAY+SILT: fine particle-size fraction (the sum of clay and silt content); C:N: organic carbon to total nitrogen ratio; CEC: cation exchange capacity of the soil; pH: soil pH. *$P < 0.001$.

In different biomes and soil depths, the effects of MAT and MAP show different magnitudes or even opposite directions (Fig. 5a,b). Although a general negative effect of MAT on τ has been found in a previous meta-analysis (Chen et al., 2013), our results show that such effect was reduced and even changed to be positive in tropical regions (Fig. 5a). This can be attributed to the contrasting in relationship of NPP with temperature between tropical and extratropical regions, which stem from their distinct limiting factors affecting plant growth (Fig. S25) (Chapin et al., 2011; Slot and Winter, 2016). In addition, the effect of MAP on τ was not significantly linear at the global scale. This is inconsistent with a previously detected negative relationship (Schimel et al., 1994; Chen et al., 2013), but supports a recent global study that detected a nonlinear relationship between τ and hydrometeorological conditions (Fan et al., 2022). Such previous discrepancies can be explained by contrasting the effects of MAP across different biomes (Fig. 5b). While warm forests and croplands exhibit significant

https://doi.org/10.5194/essd-2024-618
Preprint. Discussion started: 21 January 2025
© Author(s) 2025. CC BY 4.0 License.


positive effects, the notable negative effects are shown in tropical savannahs and grasslands, and arid regions. Additionally, it shows MAP negatively impacted subsoil τ in both boreal forests and temperate grassland and shrublands, but this effect was not significant for topsoil. These τ–climate patterns highlight the nonlinear effects of temperature and water availability on τ globally and the different driving mechanisms across biomes.

Our analyses further revealed that soil physical and chemical properties have comparable or greater effects on τ than climatic effects at global and biome scales (Fig. 5c-f). For soil physical properties as represented by the CLAY+SILT, the fraction of fine particle-size in soils was positively related with τ in general (Fig. 5c). This is mainly because that soils dominated by finer particles tend to stabilize SOC by physical and organo-mineral stabilization mechanisms, while the well-drained sandy soils generally providing limited protection of SOC against microbial decomposition (Krull et al., 2003; Lützow et al., 2006; Cotrufo et al., 2019). The relatively higher effects of CLAY+SILT on subsoil τ than that on topsoil τ (except for croplands) further indicate that mineral-associated and physically protected SOC in deep layer may plays a crucial role in stabilizing SOC stocks, and consequently decrease its climate sensitivity (Gillabel et al., 2010; Qin et al., 2019).

Among the effects of soil chemical properties, the C:N ratio plays a key role in regulating subsoil τ, ranking as the most influential soil factor (Fig. S24a). The positive impact of C:N was observed in all biomes for subsoil and specifically in boreal forests, temperate grasslands, deserts, and tundra for topsoil (Fig. 5d). However, the effects of C:N were not found significant for topsoil τ, and it even shows a negative impact in tropical and cropland regions. This finding implies that, in general, nutrient limitations decrease soil respiration and extend carbon residence time by favouring the establishment of slow-decomposing organisms or reducing organic matter quality (Crowther et al., 2019b; Li et al., 2012; Zhou et al., 2007). Whilst this effect is pronounced in the subsoil layer, it cannot be straightforwardly generalized to the topsoil in tropics and human-impacted regions. The factor of CEC showed a generally positive impact on τ in forests and croplands, but its effect was weaker in other biomes (Fig. 5e). Soil pH shows a non-significant linear correlation with τ globally, yet it exhibits divergent influences across different biomes and soil depths (Fig. 5f). It has a positive impact on τ in warm forests and on subsoil τ in temperate grasslands and croplands. Conversely, in boreal forests, tropical grasslands, and arid regions, it more negatively impacts τ in topsoil.

3.3.2 Interactive effects of climatic and edaphic factors on τ

The detected relationships between environmental factors and τ prompted us to delve deeper into the nonlinear driving mechanisms. We aimed to uncover potential interactions among the primary climatic and edaphic drivers that might be masked by analyzing the directional effects of only a single variable. We illustrate how fluctuations in one climatic variable (MAT or MAP) related with changes in another climatic variable (Fig. 6a,f) and four key soil properties (Fig. 6b-e, g-j). We found that the negative effect of MAT on τ was magnified with decreasing MAP (when MAP < 1500 mm). Meanwhile, it also shows that MAT effect on τ changed to be smaller, even can be positive for subsoil, with increasing MAP (when MAP >

https://doi.org/10.5194/essd-2024-618
Preprint. Discussion started: 21 January 2025
© Author(s) 2025. CC BY 4.0 License.

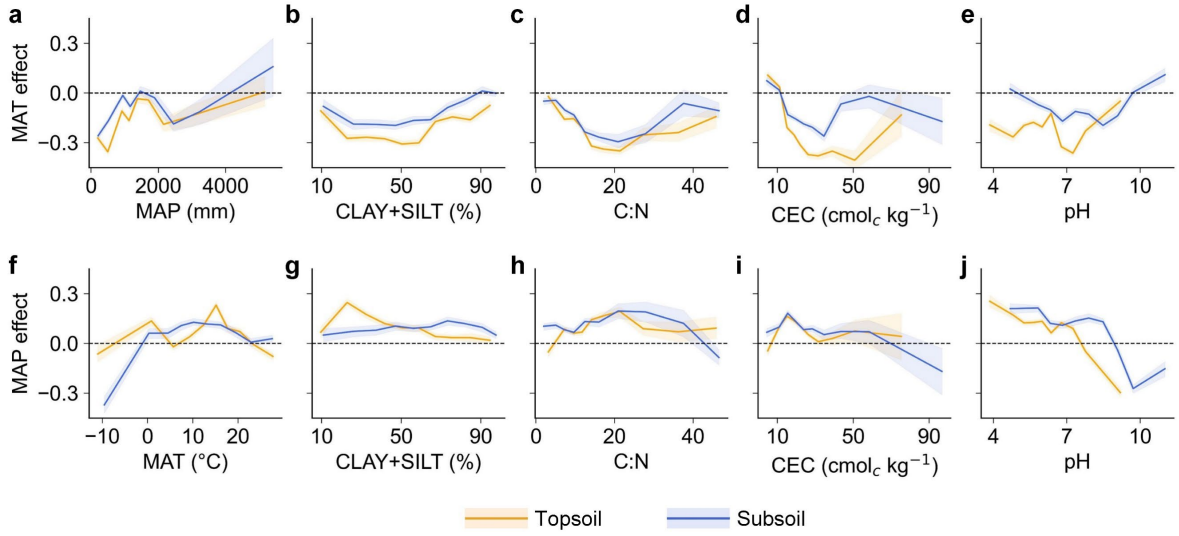

Figure 6: The climatic effects on top- and subsoil organic carbon turnover time (τ) interacted by other factors. The lines show the mean annual temperature (MAT) effect and mean annual precipitation (MAP) effect on τ in response to another climatic variable and four important soil physio-chemical (including the fine particle-size fraction [CLAY+SILT], carbon-to-nitrogen ratio [C:N], cation exchange capacity [CEC] and soil pH) variables. The variables on the *x*-axis can be considered as "interactive factors", which influence the MAT and MAP effect on τ. The values on the lines above or below dashed horizontal lines indicate the positive or negative climatic effect on top- or subsoil τ in response to the corresponding values of interactive factors. The shaded areas on the lines represent confidence intervals for the results of partial correlation analysis.

Beyond the interplay of climatic factors, soil property values significantly modulated the effects of MAT and MAP on τ. For instance, as CLAY+SILT content decreased, the negative impact of MAT was pronounced (Fig. 6b). The MAP effect was also accentuated in sandy soils but it is restricted to the topsoil layer (Fig. 6g). This result suggests that the finer soil texture may reduce carbon turnover sensitivity to temperature or water fluctuations (Krull et al., 2003). Among the interactions of soil chemical properties with climatic impacts on τ, it is evident that extremely low or high C:N ratios in soils lead to smaller climatic effects on τ (Fig. 6c,h), suggesting that the sensitivity of τ to climate is strongly influenced by whether the C:N ratio falls within an optimal range. The negative impacts of temperature was intensified with rising CEC (when CEC < 40 $cmol_c$ kg^{-1}) (Fig. 6d), mainly because higher CEC typically enhances the nutrient-supplying capacity of soils, thus quickening carbon turnover in warm conditions (Crowther et al., 2019a). The influence of soil pH on MAT effects on τ demonstrated a strong nonlinear trend. A more pronounced negative MAT effect was found when soil pH is neutral for topsoil and mildly alkaline for subsoil (Fig. 6e). This is related to that microorganism has a physiologic optimum pH (Rousk et al., 2010; Don et al., 2017), and results in the warmer temperature significantly accelerate SOC turnover rate when pH is within an optimum range (Frostegård et al., 2022; Xiang et al., 2023). Nevertheless, there is currently a need to further explore reasons explaining these pH ranges are different with soil depth, as well as its species-specificity (Bahram et al., 2018). The impact of MAP appears to be more positive in acidic soils, but becomes negative when soil pH exceeds 8 and 9

https://doi.org/10.5194/essd-2024-618
Preprint. Discussion started: 21 January 2025
© Author(s) 2025. CC BY 4.0 License.

for topsoil and subsoil, respectively (Fig. 6j). The positive MAP effect on turnover time under acidic conditions could be partly explained by the enhanced effect of increased moisture on soil weathering processes (Porras et al., 2017). Under alkaline conditions, which are mostly in dry climates (Slessarev et al., 2016), the negative MAP effect may arise from the intensified microbial transformation of plant-derived organic matter as these soils provide the favorable pH and moisture to microorganisms (Yang et al., 2022).

3.3.3 Distributions of dominating factors of τ at local scales over the world

We further analyzed the effects of these covariates by generating τ–environment models from data at sampling locations within different local areas to assess the deviation of regional patterns from that in the large scale. Overall, we find that the dominant factors controlling τ vary across different local areas (Fig. 7a,b). Across approximately 41% of the land surface area, climatic factors are the predominant controller of topsoil τ (Table 2). However, for subsoil τ, climatic factors predominantly mediate the variation of τ in only 29% of global areas. It is noteworthy that, in 57% of the global area, soil characteristics were the dominant driver of subsoil τ. Overall, soil chemical properties had a larger effect than soil physical properties. It is particularly notable in parts of tropical forests of the Amazon, the broadleaf forests spanning from eastern Indian to southeast Asia, the most parts of North America, central European, and the grasslands, deserts and xeric shrublands scattered across Africa and Australia (Fig. 7b). This phenomenon is related with previous studies suggesting that nutrient availability for soils and vegetation greatly affects τ (Cleveland and Townsend, 2006; Carvalhais et al., 2014). The contributions of four categories of environmental factors from the local-scale analysis differed less in subsoil compared to that in topsoil (Fig. 7c,d and Table 2).

Table 2. Statistical summary of the local-scale analytical results of variable (classified into four categories) importance on influencing top- and subsoil organic carbon turnover time (τ) at the local scales.

Category of variables influencing τ	Mean importance of a certain category of variables influencing τ at the local scale		Percentage of global areas that τ dominated by a certain category of variables at the local scale	
	Topsoil	Subsoil	Topsoil	Subsoil
Climate	0.37	0.20	41%	29%
Soil physical properties	0.21	0.29	18%	16%
Soil chemical properties	0.28	0.17	29%	41%
Topography	0.17	0.18	12%	14%

https://doi.org/10.5194/essd-2024-618
Preprint. Discussion started: 21 January 2025
© Author(s) 2025. CC BY 4.0 License.

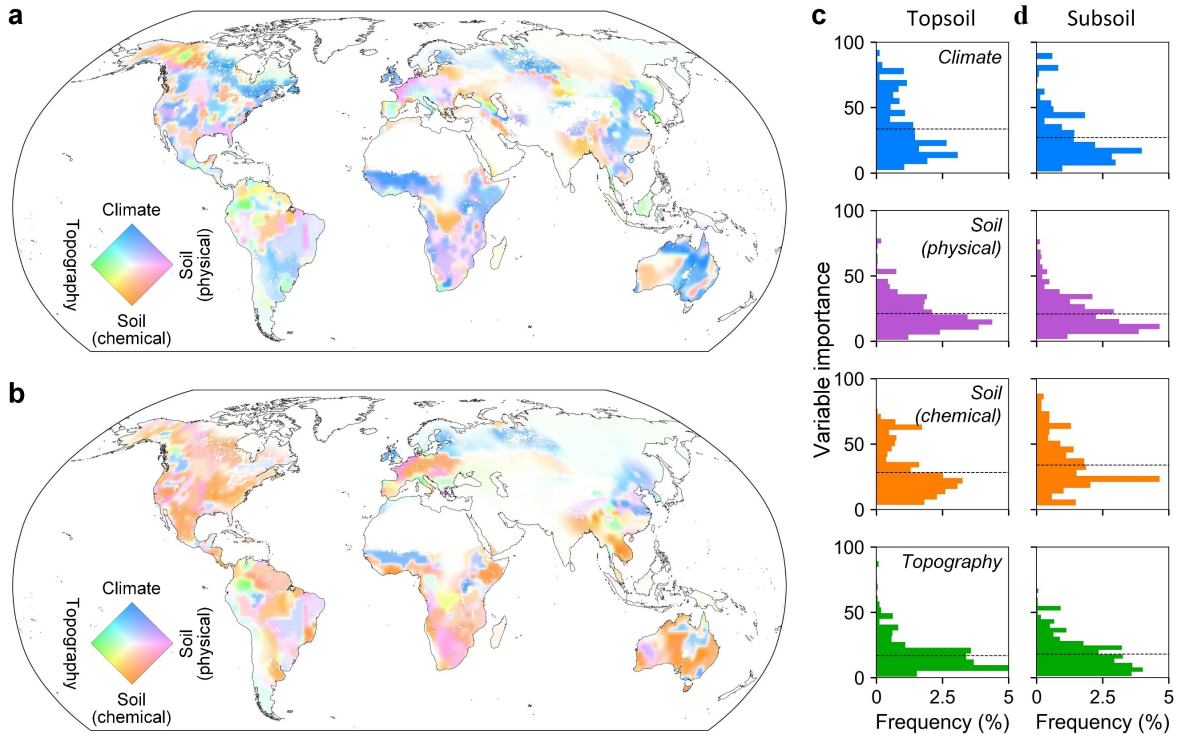

Figure 7: Local-level analysis of dominating factors of top- and subsoil organic carbon turnover time (τ). Global maps of dominant factors controlling τ in top- (**a**) and subsoil (**b**) at the local scales. Maps were created by interpolating all results of factor importance from modelling using the sample data within each local area stratified by the ecoregion map. The lighter color would be displayed if the reliability of the local result is low with a smaller number of available samples for analysis. Histograms of the local-level percentage contribution of each variable category in controlling top- (**c**) and subsoil (**d**) τ across all local areas, respectively. Dashed lines represent the mean values.

3.4 Comparison with τ from Earth system models

Our observation-based τ estimates can help constrain biogeochemical simulations by ESMs, and will be useful to improve predictions of current and future carbon cycle dynamics. While the comparison of our empirical estimates with τ estimates from ESM projections based on CMIP6 showed broad agreement in the spatial patterns of τ (Pearson'$r = 0.53$, $P < 0.001$), it highlighted that ESMs likely underestimate τ across the majority of the globe (Fig. 8a). The soil carbon turnover times estimated from ESMs were on average more than two times shorter than our data-derived (using ground-sourced samples integrated with remote sensing observations) τ estimates (Table S3). This discrepancy was particularly pronounced in tropical forests, grasslands and tundra areas (Table S4). In ~30% of the global land grids, the τ estimates from ESMs did not fall into the 90% estimation intervals of our data-driven estimates, and ~92% of global land area with a mean underestimation bias (ESM-derived τ < data-derived τ) (Fig. 8a, Table S3).

The discrepancies between τ from observations and from ESMs are also reflected in their associations with climate variables. The ESMs predicted stronger correlations with temperature and precipitation compared to our τ estimates (Fig.

https://doi.org/10.5194/essd-2024-618
Preprint. Discussion started: 21 January 2025
© Author(s) 2025. CC BY 4.0 License.

8b,c). Additionally, there were notable differences in the climate correlations between topsoil and subsoil, which ESMs do not yet capture. These findings emphasize that other factors, such as soil physico-chemical properties and soil depth, need to be accounted for in models to accurately project global soil carbon dynamics.

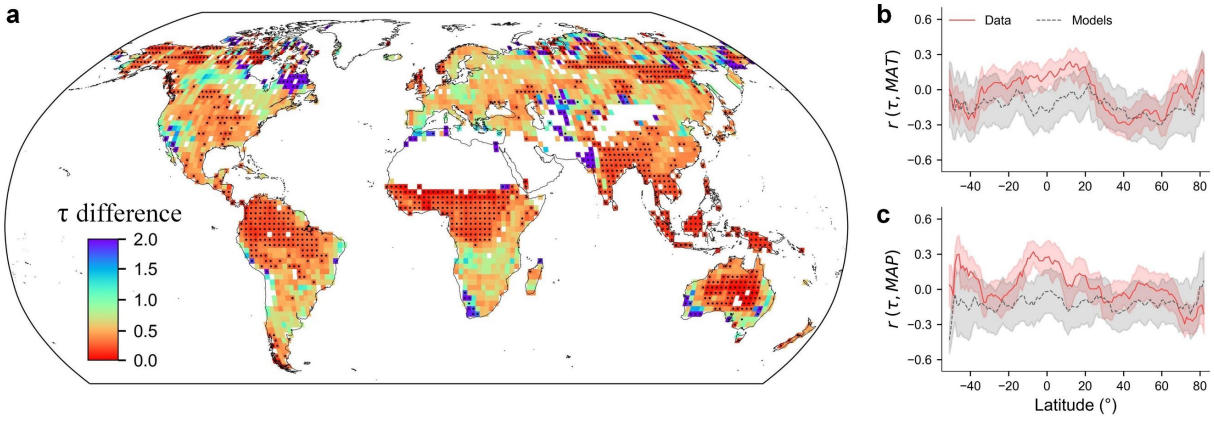

Figure 8: Comparisons of soil organic carbon turnover times (τ) from our data-derived estimates and from Earth system models (ESMs). a, Biases in τ represented by ratios of between data-derived to model-derived values across the global grid cells. Black points indicate locations where τ from ESMs are outside the 0.05 and 0.95 quantiles from the prediction uncertainty in our data-derived estimations. **b**, **c**, Comparisons of associations of data- and models (ESMs)-derived τ to mean annual temperature (MAT) (**b**) and mean annual precipitation (MAP) (**c**) along latitude gradients. The *y*-axis shows partial correlations (*r*) of τ with two climate factors, controlling for precipitation when calculating the correlation between τ and temperature (and vice versa).

3.5 Implications and future perspective

Our quantitative maps of SOC turnover times in top- and subsoil layers based on an extensive soil profile dataset represents a key step towards a better understanding of global soil carbon stocks and dynamics. Our research illustrates how global variations in τ for both top- and subsoil layers are influenced by the interplay of climatic and edaphic factors, and demonstrates their pronounced heterogeneity within and across biogeographic zones. These analyses revealed complex interactions between temperature, water availability and soil physio-chemical properties, thereby enriching our comprehension of the complex mechanisms driving spatial variability and nonlinearity in τ–environment relationships from global to local scales. The distinct factors driving τ in topsoil versus subsoil underscore the importance of incorporating soil depth when assessing large-scale τ patterns.

The findings in this study also have the potential to improve the parameterization and future projections of ESMs by integrating more accurate global τ data. Our results support several previous studies that also identified an underestimation of SOC turnover times in ESMs through ^{14}C observations (He et al., 2016; Shi et al., 2020). This discrepancy between data- and model-derived τ emphasizes the need to incorporate more detailed edaphic-climate dependent and depth-specific τ estimates into biogeochemical models to enhance predictive accuracy. Furthermore, there is evidence that the most exchange of soil carbon with the atmosphere occurs through relatively small and fast soil carbon pools on a short timescale, which can result in a “leaky sink” response when carbon input is elevated (Bradford, 2017; van Groenigen et al., 2017). This response may

https://doi.org/10.5194/essd-2024-618
Preprint. Discussion started: 21 January 2025
© Author(s) 2025. CC BY 4.0 License.


conceal the longer turnover times in inert pools that are not precisely captured by models. Adjusting turnover rates and carbon transfer parameters in ESMs to align with the longer τ values we report here may extend the turnover time of "slow" or "passive" pools in models (especially for deep layers) that constitute the majority of soil carbon (Torn et al., 2009; He et al., 2016).

To improve the accuracy of carbon cycle models and enhance the projections of future soil carbon sequestration rate and magnitude, it is essential to incorporate edaphic-climatic dependent and depth-resolved estimates of turnover times into these models. These insights across various climate zones, biomes, terrains, and soil properties contribute to reducing uncertainties related to context-dependent effects governing soil carbon stocks and dynamics, thus helping to inform strategies that enhance sustainable soil management and mitigate the impacts of climate change.

4 Data availability

The global maps of top- and subsoil organic carbon turnover times are available online at: https://doi.org/10.5281/zenodo.14560239 (Zhang, 2025).

5 Code availability

The code used for this study is publicly available at: https://github.com/leizhang-geo/global_soil_carbon_turnover_time.git.

6 Conclusions

This study provides a comprehensive assessment of global apparent SOC turnover times in both top- and subsoil layers. By integrating state-of-the-art datasets of soil profiles, plant roots, satellite observations, we employed machine learning models to produce the spatially-explicit maps of τ with quantified uncertainties. The results reveal pronounced spatial heterogeneity and non-linearity in τ–environment relationships within and among different biomes and climatic zones. Our findings demonstrate the context-dependent effects of temperature and water availability on τ, which vary depending on soil attributes, mainly including soil texture, carbon-to-nitrogen ratio, cation exchange capacity and soil pH. Considering the potentially large differences in the driving factors of τ from large to small scales, we further mapped the dominating factors of τ in two soil layers at local scales. Overall, this study synthesizes the multiple observation-based datasets that currently available, and provides new global maps of top- and subsoil organic carbon turnover times. The dataset and new insights of this study are expected to serve as a foundation for benchmarking biogeochemical models and supporting effective carbon management.

https://doi.org/10.5194/essd-2024-618
Preprint. Discussion started: 21 January 2025
© Author(s) 2025. CC BY 4.0 License.

Author contributions

L.Z. and L.Y. conceived the research; L.Z. collected the data and performed the analyses; L.Z., L.Y., T.W.C., C.M.Z., and C.Z. interpreted the analytical results with reviews from all authors; S.D. contributed to the validation and comparison with radiocarbon measurements; G.B.M.H., A.M.J.-C.W., A.-X.Z. and C.Z. contributed to global mapping and uncertainty analysis. L.Z., Y.P., and F.S. contributed to data curation and validation. L.Z., L.Y., T.W.C., and C.M.Z. wrote the paper with substantial contributions from all of the authors.

Competing interests

The authors declare that they have no conflict of interest.

Acknowledgements

The authors express sincere gratitude to Weimin Ju (International Institute for Earth System Science at Nanjing University), Nuno Carvalhais (Max Planck Institute for Biogeochemistry), Alison M. Hoyt (Earth System Science at Stanford University) and Julian Helfenstein (Soil Geography and Landscape Group at Wageningen University), whose valuable comments and suggestions on an earlier version of our manuscript.

Financial support

This work was supported by the National Natural Science Foundation of China (41971054), the Fundamental Research Funds for the Central Universities (0209-14380115), the Leading Funds for the First-Class Universities (020914912203 and 020914902302), and the Research Funds for the Frontiers Science Center for Critical Earth Material Cycling, Nanjing University. T.W.C acknowledges support from DOB Ecology and Bernina Foundation. C.M.Z was funded by the Ambizione grant PZ00P3_193646. L.Z. acknowledges the support from the U.S. Department of Energy, Office of Science, Office of Biological and Environmental Research, Terrestrial Ecosystem Science Program, in the Belowground Biogeochemistry Scientific Focus Area, under Award Number DE-AC02-05CH11231.

References

Altmann, A., Toloşi, L., Sander, O., and Lengauer, T.: Permutation importance: a corrected feature importance measure, Bioinformatics, 26, 1340–1347, https://doi.org/10.1093/bioinformatics/btq134, 2010.

Arrouays, D., McBratney, A., Minasny, B., Hempel, J., Heuvelink, G., MacMillan, R., Hartemink, A., Lagacherie, P., and McKenzie, N.: The GlobalSoilMap project specifications, in: GlobalSoilMap, edited by: Arrouays, D., McKenzie, N., Hempel, J., de Forges, A., and McBratney, A., CRC Press, 9–12, https://doi.org/10.1201/b16500-4, 2014.

© Author(s) 2025. CC BY 4.0 License.

Bahram, M., Hildebrand, F., Forslund, S. K., Anderson, J. L., Soudzilovskaia, N. A., Bodegom, P. M., Bengtsson-Palme, J., Anslan, S., Coelho, L. P., Harend, H., Huerta-Cepas, J., Medema, M. H., Maltz, M. R., Mundra, S., Olsson, P. A., Pent, M., Põlme, S., Sunagawa, S., Ryberg, M., Tedersoo, L., and Bork, P.: Structure and function of the global topsoil microbiome, Nature, 560, 233–237, https://doi.org/10.1038/s41586-018-0386-6, 2018.

Balesdent, J., Basile-Doelsch, I., Chadoeuf, J., Cornu, S., Derrien, D., Fekiacova, Z., and Hatté, C.: Atmosphere–soil carbon transfer as a function of soil depth, Nature, 559, 599–602, https://doi.org/10.1038/s41586-018-0328-3, 2018.

Bardgett, R. D., Mommer, L., and Vries, F. T. D.: Going underground: root traits as drivers of ecosystem processes, Trends in Ecology & Evolution, 29, 692–699, https://doi.org/10.1016/j.tree.2014.10.006, 2014.

Batjes, N. H.: Total carbon and nitrogen in the soils of the world, Eur J Soil Science, 47, 151–163, https://doi.org/10.1111/j.1365-2389.1996.tb01386.x, 1996.

Batjes, N. H., Ribeiro, E., and Van Oostrum, A.: Standardised soil profile data to support global mapping and modelling (WoSIS snapshot 2019), Earth System Science Data, 12, 299–320, https://doi.org/10.5194/essd-12-299-2020, 2020.

Bishop, T. F. A., McBratney, A. B., and Laslett, G. M.: Modelling soil attribute depth functions with equal-area quadratic smoothing splines, Geoderma, 91, 27–45, https://doi.org/10.1016/S0016-7061(99)00003-8, 1999.

Braakhekke, M. C., Beer, C., Hoosbeek, M. R., Reichstein, M., Kruijt, B., Schrumpf, M., and Kabat, P.: SOMPROF: A vertically explicit soil organic matter model, Ecological Modelling, 222, 1712–1730, https://doi.org/10.1016/j.ecolmodel.2011.02.015, 2011.

Bradford, M. A.: A leaky sink, Nature Clim Change, 7, 475–476, https://doi.org/10.1038/nclimate3332, 2017.

Brady, N. C. and Weil, R. R.: The nature and properties of soils, 12th ed., Prentice Hall, Upper Saddle River, N.J, 881 pp., 1999.

Breiman, L.: Random Forests, Machine Learning, 45, 5–32, https://doi.org/10.1023/a:1010933404324, 2001.

Carvalhais, N., Forkel, M., Khomik, M., Bellarby, J., Jung, M., Migliavacca, M., Mu, M., Saatchi, S., Santoro, M., Thurner, M., Weber, U., Ahrens, B., Beer, C., Cescatti, A., Randerson, J. T., and Reichstein, M.: Global covariation of carbon turnover times with climate in terrestrial ecosystems, Nature, 514, 213–217, https://doi.org/10.1038/nature13731, 2014.

Chapin, F. S., Matson, P. A., and Vitousek, P. M.: Principles of Terrestrial Ecosystem Ecology, Springer New York, New York, NY, https://doi.org/10.1007/978-1-4419-9504-9, 2011.

Chen, J., Luo, Y., and Sinsabaugh, R. L.: Subsoil carbon loss, Nat. Geosci., 16, 284–285, https://doi.org/10.1038/s41561-023-01164-9, 2023.

Chen, L., Fang, K., Wei, B., Qin, S., Feng, X., Hu, T., Ji, C., and Yang, Y.: Soil carbon persistence governed by plant input and mineral protection at regional and global scales, Ecology Letters, 24, 1018–1028, https://doi.org/10.1111/ele.13723, 2021.

Chen, S., Huang, Y., Zou, J., and Shi, Y.: Mean residence time of global topsoil organic carbon depends on temperature, precipitation and soil nitrogen, Global and Planetary Change, 100, 99–108, https://doi.org/10.1016/j.gloplacha.2012.10.006, 2013.

Cleveland, C. C. and Townsend, A. R.: Nutrient additions to a tropical rain forest drive substantial soil carbon dioxide losses to the atmosphere, Proceedings of the National Academy of Sciences, 103, 10316–10321, https://doi.org/10.1073/pnas.0600989103, 2006.

Cotrufo, M. F., Ranalli, M. G., Haddix, M. L., Six, J., and Lugato, E.: Soil carbon storage informed by particulate and mineral-associated organic matter, Nat. Geosci., 12, 989–994, https://doi.org/10.1038/s41561-019-0484-6, 2019.

Crowther, T. W., Todd-Brown, K. E. O., Rowe, C. W., Wieder, W. R., Carey, J. C., Machmuller, M. B., Snoek, B. L., Fang, S., Zhou, G., Allison, S. D., Blair, J. M., Bridgham, S. D., Burton, A. J., Carrillo, Y., Reich, P. B., Clark, J. S., Classen, A. T., Dijkstra, F. A., Elberling,

© Author(s) 2025. CC BY 4.0 License.

B., Emmett, B. A., Estiarte, M., Frey, S. D., Guo, J., Harte, J., Jiang, L., Johnson, B. R., Kröel-Dulay, G., Larsen, K. S., Laudon, H., Lavallee, J. M., Luo, Y., Lupascu, M., Ma, L. N., Marhan, S., Michelsen, A., Mohan, J., Niu, S., Pendall, E., Peñuelas, J., Pfeifer-Meister, L., Poll, C., Reinsch, S., Reynolds, L. L., Schmidt, I. K., Sistla, S., Sokol, N. W., Templer, P. H., Treseder, K. K., Welker, J. M., and Bradford, M. A.: Quantifying global soil carbon losses in response to warming, Nature, 540, 104–108, https://doi.org/10.1038/nature20150, 2016.

Crowther, T. W., Riggs, C., Lind, E. M., Borer, E. T., Seabloom, E. W., Hobbie, S. E., Wubs, J., Adler, P. B., Firn, J., Gherardi, L., Hagenah, N., Hofmockel, K. S., Knops, J. M. H., McCulley, R. L., MacDougall, A. S., Peri, P. L., Prober, S. M., Stevens, C. J., and Routh, D.: Sensitivity of global soil carbon stocks to combined nutrient enrichment, Ecology Letters, 22, 936–945, https://doi.org/10.1111/ele.13258, 2019a.

Crowther, T. W., van den Hoogen, J., Wan, J., Mayes, M. A., Keiser, A. D., Mo, L., Averill, C., and Maynard, D. S.: The global soil community and its influence on biogeochemistry, Science, 365, eaav0550, https://doi.org/10.1126/science.aav0550, 2019b.

Davidson, E. A. and Janssens, I. A.: Temperature sensitivity of soil carbon decomposition and feedbacks to climate change, Nature, 440, 165–173, https://doi.org/10.1038/nature04514, 2006.

Dinerstein, E., Olson, D., Joshi, A., Vynne, C., Burgess, N. D., Wikramanayake, E., Hahn, N., Palminteri, S., Hedao, P., Noss, R., Hansen, M., Locke, H., Ellis, E. C., Jones, B., Barber, C. V., Hayes, R., Kormos, C., Martin, V., Crist, E., Sechrest, W., Price, L., Baillie, J. E. M., Weeden, D., Suckling, K., Davis, C., Sizer, N., Moore, R., Thau, D., Birch, T., Potapov, P., Turubanova, S., Tyukavina, A., de Souza, N., Pintea, L., Brito, J. C., Llewellyn, O. A., Miller, A. G., Patzelt, A., Ghazanfar, S. A., Timberlake, J., Klöser, H., Shennan-Farpón, Y., Kindt, R., Lillesø, J.-P. B., van Breugel, P., Graudal, L., Voge, M., Al-Shammari, K. F., and Saleem, M.: An Ecoregion-Based Approach to Protecting Half the Terrestrial Realm, BioScience, 67, 534–545, https://doi.org/10.1093/biosci/bix014, 2017.

Doetterl, S., Stevens, A., Six, J., Merckx, R., Van Oost, K., Casanova Pinto, M., Casanova-Katny, A., Muñoz, C., Boudin, M., Zagal Venegas, E., and Boeckx, P.: Soil carbon storage controlled by interactions between geochemistry and climate, Nature Geosci, 8, 780–783, https://doi.org/10.1038/ngeo2516, 2015.

Doetterl, S., Berhe, A. A., Nadeu, E., Wang, Z., Sommer, M., and Fiener, P.: Erosion, deposition and soil carbon: A review of process-level controls, experimental tools and models to address C cycling in dynamic landscapes, Earth-Science Reviews, 154, 102–122, https://doi.org/10.1016/j.earscirev.2015.12.005, 2016.

Don, A., Böhme, I. H., Dohrmann, A. B., Poeplau, C., and Tebbe, C. C.: Microbial community composition affects soil organic carbon turnover in mineral soils, Biol Fertil Soils, 53, 445–456, https://doi.org/10.1007/s00374-017-1198-9, 2017.

Fan, N., Koirala, S., Reichstein, M., Thurner, M., Avitabile, V., Santoro, M., Ahrens, B., Weber, U., and Carvalhais, N.: Apparent ecosystem carbon turnover time: uncertainties and robust features, Earth System Science Data, 12, 2517–2536, https://doi.org/10.5194/essd-12-2517-2020, 2020.

Fan, N., Reichstein, M., Koirala, S., Ahrens, B., Mahecha, M. D., and Carvalhais, N.: Global apparent temperature sensitivity of terrestrial carbon turnover modulated by hydrometeorological factors, Nat. Geosci., 15, 989–994, https://doi.org/10.1038/s41561-022-01074-2, 2022.

FAO–Unesco: Soil map of the world, FAO, Rome, Italy, 1990.

Field, C. B., Barros, V. R., and Intergovernmental Panel on Climate Change (Eds.): Climate change 2014: impacts, adaptation, and vulnerability: Working Group II contribution to the fifth assessment report of the Intergovernmental Panel on Climate Change, Cambridge University Press, New York, NY, 1 pp., 2014.

Friend, A. D., Lucht, W., Rademacher, T. T., Keribin, R., Betts, R., Cadule, P., Ciais, P., Clark, D. B., Dankers, R., Falloon, P. D., Ito, A., Kahana, R., Kleidon, A., Lomas, M. R., Nishina, K., Ostberg, S., Pavlick, R., Peylin, P., Schaphoff, S., Vuichard, N., Warszawski, L., Wiltshire, A., and Woodward, F. I.: Carbon residence time dominates uncertainty in terrestrial vegetation responses to future climate and atmospheric CO2, Proceedings of the National Academy of Sciences, 111, 3280–3285, https://doi.org/10.1073/pnas.1222477110, 2014.

© Author(s) 2025. CC BY 4.0 License.

Frostegård, Å., Vick, S. H. W., Lim, N. Y. N., Bakken, L. R., and Shapleigh, J. P.: Linking meta-omics to the kinetics of denitrification intermediates reveals pH-dependent causes of N2O emissions and nitrite accumulation in soil, ISME J, 16, 26–37, https://doi.org/10.1038/s41396-021-01045-2, 2022.

Gale, M. R. and Grigal, D. F.: Vertical root distributions of northern tree species in relation to successional status, Can. J. For. Res., 17, 829–834, https://doi.org/10.1139/x87-131, 1987.

Giardina, C. P. and Ryan, M. G.: Evidence that decomposition rates of organic carbon in mineral soil do not vary with temperature, Nature, 404, 858–861, https://doi.org/10.1038/35009076, 2000.

Gillabel, J., Cebrian-Lopez, B., Six, J., and Merckx, R.: Experimental evidence for the attenuating effect of SOM protection on temperature sensitivity of SOM decomposition, Global Change Biology, 16, 2789–2798, https://doi.org/10.1111/j.1365-2486.2009.02132.x, 2010.

Goovaerts, P.: Geostatistical modelling of uncertainty in soil science, Geoderma, 103, 3–26, https://doi.org/10.1016/S0016-7061(01)00067-2, 2001.

Gower, S. T., Kucharik, C. J., and Norman, J. M.: Direct and Indirect Estimation of Leaf Area Index, fAPAR, and Net Primary Production of Terrestrial Ecosystems, Remote Sensing of Environment, 70, 29–51, https://doi.org/10.1016/S0034-4257(99)00056-5, 1999.

van Groenigen, K. J., Osenberg, C. W., Terrer, C., Carrillo, Y., Dijkstra, F. A., Heath, J., Nie, M., Pendall, E., Phillips, R. P., and Hungate, B. A.: Faster turnover of new soil carbon inputs under increased atmospheric CO2, Global Change Biology, 23, 4420–4429, https://doi.org/10.1111/gcb.13752, 2017.

Guerrero-Ramírez, N. R., Mommer, L., Freschet, G. T., Iversen, C. M., McCormack, M. L., Kattge, J., Poorter, H., van der Plas, F., Bergmann, J., Kuyper, T. W., York, L. M., Bruelheide, H., Laughlin, D. C., Meier, I. C., Roumet, C., Semchenko, M., Sweeney, C. J., van Ruijven, J., Valverde-Barrantes, O. J., Aubin, I., Catford, J. A., Manning, P., Martin, A., Milla, R., Minden, V., Pausas, J. G., Smith, S. W., Soudzilovskaia, N. A., Ammer, C., Butterfield, B., Craine, J., Cornelissen, J. H. C., de Vries, F. T., Isaac, M. E., Kramer, K., König, C., Lamb, E. G., Onipchenko, V. G., Peñuelas, J., Reich, P. B., Rillig, M. C., Sack, L., Shipley, B., Tedersoo, L., Valladares, F., van Bodegom, P., Weigelt, P., Wright, J. P., and Weigelt, A.: Global root traits (GRooT) database, Global Ecology and Biogeography, 30, 25–37, https://doi.org/10.1111/geb.13179, 2021.

Han, D., Hu, Z., Wang, X., Wang, T., Chen, A., Weng, Q., Liang, M., Zeng, X., Cao, R., Di, K., Luo, D., Zhang, G., Yang, Y., He, H., Fan, J., and Yu, G.: Shift in controlling factors of carbon stocks across biomes on the Qinghai-Tibetan Plateau, Environ. Res. Lett., 17, 074016, https://doi.org/10.1088/1748-9326/ac78f5, 2022.

He, Y., Trumbore, S. E., Torn, M. S., Harden, J. W., Vaughn, L. J. S., Allison, S. D., and Randerson, J. T.: Radiocarbon constraints imply reduced carbon uptake by soils during the 21st century, Science, 353, 1419–1424, https://doi.org/10.1126/science.aad4273, 2016.

Heuvelink, G. B. M.: Error Propagation in Environmental Modelling with GIS, CRC Press, London, 150 pp., https://doi.org/10.4324/9780203016114, 1998.

Hicks Pries, C., Ryals, R., Zhu, B., Min, K., Cooper, A., Goldsmith, S., Pett-Ridge, J., Torn, M., and Asefaw Berhe, A.: The Deep Soil Organic Carbon Response to Global Change, Annual Review of Ecology, Evolution, and Systematics, 54, null, https://doi.org/10.1146/annurev-ecolsys-102320-085332, 2023.

Hicks Pries, C. E., Castanha, C., Porras, R. C., and Torn, M. S.: The whole-soil carbon flux in response to warming, Science, 355, 1420–1423, https://doi.org/10.1126/science.aal1319, 2017.

Holland, E. A., Post, W. M., Matthews, E. G., Sulzman, J. M., Staufer, R., and Krankina, O. N.: A Global Database of Litterfall Mass and Litter Pool Carbon and Nutrients, 2.150694 MB, https://doi.org/10.3334/ORNLDAAC/1244, 2015.

van den Hoogen, J., Geisen, S., Routh, D., Ferris, H., Traunspurger, W., Wardle, D. A., de Goede, R. G. M., Adams, B. J., Ahmad, W., Andriuzzi, W. S., Bardgett, R. D., Bonkowski, M., Campos-Herrera, R., Cares, J. E., Caruso, T., de Brito Caixeta, L., Chen, X., Costa, S.

© Author(s) 2025. CC BY 4.0 License.

R., Creamer, R., Mauro da Cunha Castro, J., Dam, M., Djigal, D., Escuer, M., Griffiths, B. S., Gutiérrez, C., Hohberg, K., Kalinkina, D., Kardol, P., Kergunteuil, A., Korthals, G., Krashevska, V., Kudrin, A. A., Li, Q., Liang, W., Magilton, M., Marais, M., Martín, J. A. R., Matveeva, E., Mayad, E. H., Mulder, C., Mullin, P., Neilson, R., Nguyen, T. A. D., Nielsen, U. N., Okada, H., Rius, J. E. P., Pan, K., Peneva, V., Pellissier, L., Carlos Pereira da Silva, J., Pitteloud, C., Powers, T. O., Powers, K., Quist, C. W., Rasmann, S., Moreno, S. S., Scheu, S., Setälä, H., Sushchuk, A., Tiunov, A. V., Trap, J., van der Putten, W., Vestergård, M., Villenave, C., Waeyenberge, L., Wall, D. H., Wilschut, R., Wright, D. G., Yang, J., and Crowther, T. W.: Soil nematode abundance and functional group composition at a global scale, Nature, 572, 194–198, https://doi.org/10.1038/s41586-019-1418-6, 2019.

Hugelius, G., Tarnocai, C., Broll, G., Canadell, J. G., Kuhry, P., and Swanson, D. K.: The Northern Circumpolar Soil Carbon Database: spatially distributed datasets of soil coverage and soil carbon storage in the northern permafrost regions, Earth System Science Data, 5, 3–13, https://doi.org/10.5194/essd-5-3-2013, 2013.

Jackson, R. B., Canadell, J., Ehleringer, J. R., Mooney, H. A., Sala, O. E., and Schulze, E. D.: A global analysis of root distributions for terrestrial biomes, Oecologia, 108, 389–411, https://doi.org/10.1007/BF00333714, 1996.

Jia, B., Zhou, G., and Xu, Z.: Forest litterfall and its composition: a new data set of observational data from China, Ecology, 97, 1365–1365, https://doi.org/10.1890/15-1604.1, 2016.

Jia, J., Cao, Z., Liu, C., Zhang, Z., Lin, L., Wang, Y., Haghipour, N., Wacker, L., Bao, H., Dittmar, T., Simpson, M. J., Yang, H., Crowther, T. W., Eglinton, T. I., He, J.-S., and Feng, X.: Climate warming alters subsoil but not topsoil carbon dynamics in alpine grassland, Global Change Biology, 25, 4383–4393, https://doi.org/10.1111/gcb.14823, 2019.

Koven, C. D., Riley, W. J., Subin, Z. M., Tang, J. Y., Torn, M. S., Collins, W. D., Bonan, G. B., Lawrence, D. M., and Swenson, S. C.: The effect of vertically resolved soil biogeochemistry and alternate soil C and N models on C dynamics of CLM4, Biogeosciences, 10, 7109–7131, https://doi.org/10.5194/bg-10-7109-2013, 2013.

Krull, E. S., Baldock, J. A., and Skjemstad, J. O.: Importance of mechanisms and processes of the stabilisation of soil organic matter for modelling carbon turnover, Functional Plant Biol., 30, 207–222, https://doi.org/10.1071/fp02085, 2003.

Li, D., Niu, S., and Luo, Y.: Global patterns of the dynamics of soil carbon and nitrogen stocks following afforestation: a meta-analysis, New Phytologist, 195, 172–181, https://doi.org/10.1111/j.1469-8137.2012.04150.x, 2012.

Liu, F., Wu, H., Zhao, Y., Li, D., Yang, J.-L., Song, X., Shi, Z., Zhu, A.-X., and Zhang, G.-L.: Mapping high resolution National Soil Information Grids of China, Science Bulletin, 67, 328–340, https://doi.org/10.1016/j.scib.2021.10.013, 2022.

Luo, Z., Feng, W., Luo, Y., Baldock, J., and Wang, E.: Soil organic carbon dynamics jointly controlled by climate, carbon inputs, soil properties and soil carbon fractions, Global Change Biology, 23, 4430–4439, https://doi.org/10.1111/gcb.13767, 2017.

Luo, Z., Wang, G., and Wang, E.: Global subsoil organic carbon turnover times dominantly controlled by soil properties rather than climate, Nat Commun, 10, 3688, https://doi.org/10.1038/s41467-019-11597-9, 2019.

Lützow, M. v., Kögel-Knabner, I., Ekschmitt, K., Matzner, E., Guggenberger, G., Marschner, B., and Flessa, H.: Stabilization of organic matter in temperate soils: mechanisms and their relevance under different soil conditions – a review, European Journal of Soil Science, 57, 426–445, https://doi.org/10.1111/j.1365-2389.2006.00809.x, 2006.

Ma, H., Mo, L., Crowther, T. W., Maynard, D. S., van den Hoogen, J., Stocker, B. D., Terrer, C., and Zohner, C. M.: The global distribution and environmental drivers of aboveground versus belowground plant biomass, Nat Ecol Evol, 1–13, https://doi.org/10.1038/s41559-021-01485-1, 2021.

Malone, B. P., McBratney, A. B., Minasny, B., and Laslett, G. M.: Mapping continuous depth functions of soil carbon storage and available water capacity, Geoderma, 154, 138–152, https://doi.org/10.1016/j.geoderma.2009.10.007, 2009.

Mathieu, J. A., Hatté, C., Balesdent, J., and Parent, É.: Deep soil carbon dynamics are driven more by soil type than by climate: a worldwide meta-analysis of radiocarbon profiles, Global Change Biology, 21, 4278–4292, https://doi.org/10.1111/gcb.13012, 2015.

© Author(s) 2025. CC BY 4.0 License.

Meinshausen, N.: Quantile Regression Forests, Journal of Machine Learning Research, 7, 983–999, 2006.

Oleson, K., Lawrence, D., Bonan, G., Drewniak, B., Huang, M., Koven, C., Levis, S., Li, F., Riley, W., Subin, Z., Swenson, S., Thornton, P., Bozbiyik, A., Fisher, R., Heald, C., Kluzek, E., Lamarque, J.-F., Lawrence, P., Leung, L., Lipscomb, W., Muszala, S., Ricciuto, D., Sacks, W., Sun, Y., Tang, J., and Yang, Z.-L.: Technical description of version 4.5 of the Community Land Model (CLM), [object Object], https://doi.org/10.5065/D6RR1W7M, 2013.

Poggio, L., de Sousa, L. M., Batjes, N. H., Heuvelink, G. B. M., Kempen, B., Ribeiro, E., and Rossiter, D.: SoilGrids 2.0: producing soil information for the globe with quantified spatial uncertainty, SOIL, 7, 217–240, https://doi.org/10.5194/soil-7-217-2021, 2021.

Porras, R. C., Hicks Pries, C. E., McFarlane, K. J., Hanson, P. J., and Torn, M. S.: Association with pedogenic iron and aluminum: effects on soil organic carbon storage and stability in four temperate forest soils, Biogeochemistry, 133, 333–345, https://doi.org/10.1007/s10533-017-0337-6, 2017.

Qin, S., Chen, L., Fang, K., Zhang, Q., Wang, J., Liu, F., Yu, J., and Yang, Y.: Temperature sensitivity of SOM decomposition governed by aggregate protection and microbial communities, Science Advances, 5, eaau1218, https://doi.org/10.1126/sciadv.aau1218, 2019.

Reichstein, M., Baldocchi, D., Running, S., Tenhunen, J., Valentini, R., Rambal, S., Ourcival, J., Granier, A., Bouriaud, O., Bernhofer, C., and Gruenwald, T.: Validation Effort of MODIS LAI/GPP/NPP Products at FLUXNET Sites, 2002, B61B-0728, 2002.

Rousk, J., Bååth, E., Brookes, P. C., Lauber, C. L., Lozupone, C., Caporaso, J. G., Knight, R., and Fierer, N.: Soil bacterial and fungal communities across a pH gradient in an arable soil, ISME J, 4, 1340–1351, https://doi.org/10.1038/ismej.2010.58, 2010.

Rumpel, C. and Kögel-Knabner, I.: Deep soil organic matter—a key but poorly understood component of terrestrial C cycle, Plant Soil, 338, 143–158, https://doi.org/10.1007/s11104-010-0391-5, 2011.

Running, S. and Zhao, M.: MOD17A3HGF MODIS/Terra Net Primary Production Gap-Filled Yearly L4 Global 500 m SIN Grid V006, https://doi.org/10.5067/MODIS/MOD17A3HGF.006, 2019.

Schenk, H. J. and Jackson, R. B.: The Global Biogeography of Roots, Ecological Monographs, 72, 311–328, https://doi.org/10.1890/0012-9615(2002)072[0311:TGBOR]2.0.CO;2, 2002.

Schenk, H. J. and Jackson, R. B.: Mapping the global distribution of deep roots in relation to climate and soil characteristics, Geoderma, 126, 129–140, https://doi.org/10.1016/j.geoderma.2004.11.018, 2005.

Schimel, D. S.: Terrestrial ecosystems and the carbon cycle, Global Change Biology, 1, 77–91, https://doi.org/10.1111/j.1365-2486.1995.tb00008.x, 1995.

Schimel, D. S., Braswell, B. H., Holland, E. A., McKeown, R., Ojima, D. S., Painter, T. H., Parton, W. J., and Townsend, A. R.: Climatic, edaphic, and biotic controls over storage and turnover of carbon in soils, Global Biogeochemical Cycles, 8, 279–293, https://doi.org/10.1029/94GB00993, 1994.

Schmidt, M. W. I., Torn, M. S., Abiven, S., Dittmar, T., Guggenberger, G., Janssens, I. A., Kleber, M., Kögel-Knabner, I., Lehmann, J., Manning, D. A. C., Nannipieri, P., Rasse, D. P., Weiner, S., and Trumbore, S. E.: Persistence of soil organic matter as an ecosystem property, Nature, 478, 49–56, https://doi.org/10.1038/nature10386, 2011.

Shi, Y., Tang, X., Yu, P., Xu, L., Chen, G., Cao, L., Song, C., Cai, C., and Li, J.: Subsoil organic carbon turnover is dominantly controlled by soil properties in grasslands across China, CATENA, 207, 105654, https://doi.org/10.1016/j.catena.2021.105654, 2021.

Shi, Z., Allison, S. D., He, Y., Levine, P. A., Hoyt, A. M., Beem-Miller, J., Zhu, Q., Wieder, W. R., Trumbore, S., and Randerson, J. T.: The age distribution of global soil carbon inferred from radiocarbon measurements, Nat. Geosci., 13, 555–559, https://doi.org/10.1038/s41561-020-0596-z, 2020.

© Author(s) 2025. CC BY 4.0 License.

Sierra, C. A., Müller, M., Metzler, H., Manzoni, S., and Trumbore, S. E.: The muddle of ages, turnover, transit, and residence times in the carbon cycle, Global Change Biology, 23, 1763–1773, https://doi.org/10.1111/gcb.13556, 2017.

Sierra, C. A., Ahrens, B., Bolinder, M. A., Braakhekke, M. C., von Fromm, S., Kätterer, T., Luo, Z., Parvin, N., and Wang, G.: Carbon sequestration in the subsoil and the time required to stabilize carbon for climate change mitigation, Global Change Biology, 30, e17153, https://doi.org/10.1111/gcb.17153, 2024.

Six, J. and Jastrow, J.: Organic Matter Turnover, Encyclopedia of Soil Science, https://doi.org/10.1201/NOE0849338304.ch252, 2002.

Slessarev, E. W., Lin, Y., Bingham, N. L., Johnson, J. E., Dai, Y., Schimel, J. P., and Chadwick, O. A.: Water balance creates a threshold in soil pH at the global scale, Nature, 540, 567–569, https://doi.org/10.1038/nature20139, 2016.

Slot, M. and Winter, K.: The Effects of Rising Temperature on the Ecophysiology of Tropical Forest Trees, in: Tropical Tree Physiology: Adaptations and Responses in a Changing Environment, edited by: Goldstein, G. and Santiago, L. S., Springer International Publishing, Cham, 385–412, https://doi.org/10.1007/978-3-319-27422-5_18, 2016.

Smith, P., Poch, R. M., Lobb, D. A., Bhattacharyya, R., Alloush, G., Eudoxie, G. D., Anjos, L. H. C., Castellano, M., Ndzana, G. M., Chenu, C., Naidu, R., Vijayanathan, J., Muscolo, A. M., Studdert, G. A., Eugenio, N. R., Calzolari, M. C., Amuri, N., and Hallett, P.: Status of the World's Soils, Annual Review of Environment and Resources, 49, 73–104, https://doi.org/10.1146/annurev-environ-030323-075629, 2024.

Soong, J. L., Castanha, C., Hicks Pries, C. E., Ofiti, N., Porras, R. C., Riley, W. J., Schmidt, M. W. I., and Torn, M. S.: Five years of whole-soil warming led to loss of subsoil carbon stocks and increased CO_2 efflux, Sci. Adv., 7, eabd1343, https://doi.org/10.1126/sciadv.abd1343, 2021.

Spawn, S. A., Sullivan, C. C., Lark, T. J., and Gibbs, H. K.: Harmonized global maps of above and belowground biomass carbon density in the year 2010, Sci Data, 7, 112, https://doi.org/10.1038/s41597-020-0444-4, 2020.

Todd-Brown, K. E. O., Randerson, J. T., Post, W. M., Hoffman, F. M., Tarnocai, C., Schuur, E. a. G., and Allison, S. D.: Causes of variation in soil carbon simulations from CMIP5 Earth system models and comparison with observations, Biogeosciences, 10, 1717–1736, https://doi.org/10.5194/bg-10-1717-2013, 2013.

Torn, M. S., Swanston, C. W., Castanha, C., and Trumbore, S. E.: Storage and Turnover of Organic Matter in Soil, in: Biophysico-Chemical Processes Involving Natural Nonliving Organic Matter in Environmental Systems, John Wiley & Sons, Ltd, 219–272, https://doi.org/10.1002/9780470494950.ch6, 2009.

Tumber-Dávila, S. J., Schenk, H. J., Du, E., and Jackson, R. B.: Plant sizes and shapes above and belowground and their interactions with climate, New Phytologist, nph.18031, https://doi.org/10.1111/nph.18031, 2022.

Varney, R. M., Chadburn, S. E., Burke, E. J., and Cox, P. M.: Evaluation of soil carbon simulation in CMIP6 Earth system models, Biogeosciences, 19, 4671–4704, https://doi.org/10.5194/bg-19-4671-2022, 2022.

Viscarra Rossel, R. A., Lee, J., Behrens, T., Luo, Z., Baldock, J., and Richards, A.: Continental-scale soil carbon composition and vulnerability modulated by regional environmental controls, Nature Geoscience, 12, 547–552, https://doi.org/10.1038/s41561-019-0373-z, 2019.

Wang, J., Sun, J., Xia, J., He, N., Li, M., and Niu, S.: Soil and vegetation carbon turnover times from tropical to boreal forests, Functional Ecology, 32, 71–82, https://doi.org/10.1111/1365-2435.12914, 2018.

Wright, M. N. and Ziegler, A.: ranger: A Fast Implementation of Random Forests for High Dimensional Data in C++ and R, Journal of Statistical Software, 77, 1–17, https://doi.org/10.18637/jss.v077.i01, 2017.

Wu, D., Liu, D., Wang, T., Ding, J., He, Y., Ciais, P., Zhang, G., and Piao, S.: Carbon turnover times shape topsoil carbon difference between Tibetan Plateau and Arctic tundra, Science Bulletin, 66, 1698–1704, https://doi.org/10.1016/j.scib.2021.04.019, 2021.

© Author(s) 2025. CC BY 4.0 License.

Xiang, D., Wang, G., Tian, J., and Li, W.: Global patterns and edaphic-climatic controls of soil carbon decomposition kinetics predicted from incubation experiments, Nat Commun, 14, 2171, https://doi.org/10.1038/s41467-023-37900-3, 2023.

Xiao, L., Wang, G., Wang, M., Zhang, S., Sierra, C. A., Guo, X., Chang, J., Shi, Z., and Luo, Z.: Younger carbon dominates global soil carbon efflux, Global Change Biology, gcb.16311, https://doi.org/10.1111/gcb.16311, 2022.

730 Xiao, L., Wang, G., Chang, J., Chen, Y., Guo, X., Mao, X., Wang, M., Zhang, S., Shi, Z., Luo, Y., Cheng, L., Yu, K., Mo, F., and Luo, Z.: Global depth distribution of belowground net primary productivity and its drivers, Global Ecology and Biogeography, 32, 1435–1451, https://doi.org/10.1111/geb.13705, 2023.

Yang, S., Jansen, B., Absalah, S., Kalbitz, K., Chunga Castro, F. O., and Cammeraat, E. L. H.: Soil organic carbon content and mineralization controlled by the composition, origin and molecular diversity of organic matter: A study in tropical alpine grasslands, Soil
735 and Tillage Research, 215, 105203, https://doi.org/10.1016/j.still.2021.105203, 2022.

Zeng, X.: Global Vegetation Root Distribution for Land Modeling, Journal of Hydrometeorology, 2, 525–530, https://doi.org/10.1175/1525-7541(2001)002<0525:GVRDFL>2.0.CO;2, 2001.

Zhang, G., Wan, Q., Zhang, F., Wu, K., Cai, C., Zhang, M., Li, D., Zhao, Y., and Yang, J.: Criteria for establishment of soil family and soil series in Chinese Soil Taxonomy, ACTA PEDOLOGICA SINICA, 50, 826–834, https://doi.org/10.11766/trxb201303180124, 2013.

740 Zhang, L.: Global maps of top- and subsoil organic carbon turnover times, https://doi.org/10.5281/ZENODO.14560239, 2025.

Zhou, Z., Sun, O. J., Huang, J., Li, L., Liu, P., and Han, X.: Soil carbon and nitrogen stores and storage potential as affected by land-use in an agro-pastoral ecotone of northern China, Biogeochemistry, 82, 127–138, https://doi.org/10.1007/s10533-006-9058-y, 2007.

Zosso, C. U., Ofiti, N. O. E., Torn, M. S., Wiesenberg, G. L. B., and Schmidt, M. W. I.: Rapid loss of complex polymers and pyrogenic carbon in subsoils under whole-soil warming, Nat. Geosci., 16, 344–348, https://doi.org/10.1038/s41561-023-01142-1, 2023.